

SEVERE WEATHER

AN ASSESSMENT OF THE NGM FOUR-LAYER LIFTED INDEX PROGNOSSES OF EXTREME INSTABILITY

Steven J. Weiss (1)
National Weather Service
National Severe Storms Forecast Center
Kansas City, Missouri 64106

ABSTRACT

The ability of the Nested Grid Model to predict conditions of extreme instability is examined. Extreme instability, defined as the occurrence of lifted index values of -8°C or less, is often associated with warm season outbreaks of severe thunderstorms. Error analysis of the 24 and 36-h model forecasts indicates that the prediction of extreme instability is nearly always overforecast. In contrast, when conditions of extreme instability actually occur, the model tends to underforecast the degree of instability. Thus, it is concluded that the NGM exhibits a very high False Alarm Ratio and a very low Probability of Detection when conditions of extreme instability are considered.

Changes in the NGM simulation of some physical processes were implemented midway through the data period, and appear to have had a noticeable affect on the stability forecasts. The magnitude of the overforecast errors increased after the revised physics package was implemented. Further, large overforecast errors were often coincident with forecast precipitation maxima, and were occasionally coincident with precipitation "bulls-eyes." It is hypothesized that the revised convective adjustment procedure is a major contributor to the instability errors, primarily due to an excessive low level latent heat release.

1. INTRODUCTION

A basic requirement for the development of thunderstorms is the presence of a moist, unstably stratified air mass (see Miller, 2; Doswell, 3; McNulty, 4). The instability of an air mass is typically assessed by evaluating a single parameter index, such as the Showalter Index (Showalter, 5) or the SELS Lifted Index (LI) described by Galway (6). These stability indices attempt to measure the buoyancy available to a lifted parcel at 500 mb, and are based upon the latest rawinsonde data. The indices can provide significant information for short-range forecasts (0-12-h period); however, their utility diminishes substantially when applied to medium-range (12-48-h period) convective forecasting.

To aid operational forecasters, numerical weather prediction models generate a variety of forecast parameters, including predictions of air mass stability. Although no direct correlation exists between thunderstorm occurrence and air mass instability, it is essential from the prognostic point of view to determine the ability of numerical models to accurately predict instability. This study focuses on the Nested Grid Model (NGM) forecasts of a version of the lifted index.

2. THE NGM LIFTED INDEX

The vertical structure of the NGM is depicted in Fig. 1. It can be seen that the thicknesses of the NGM layers provide greater resolution, particularly near the ground, compared to the Limited-area Fine Mesh (LFM) model. The NGM lifted index is

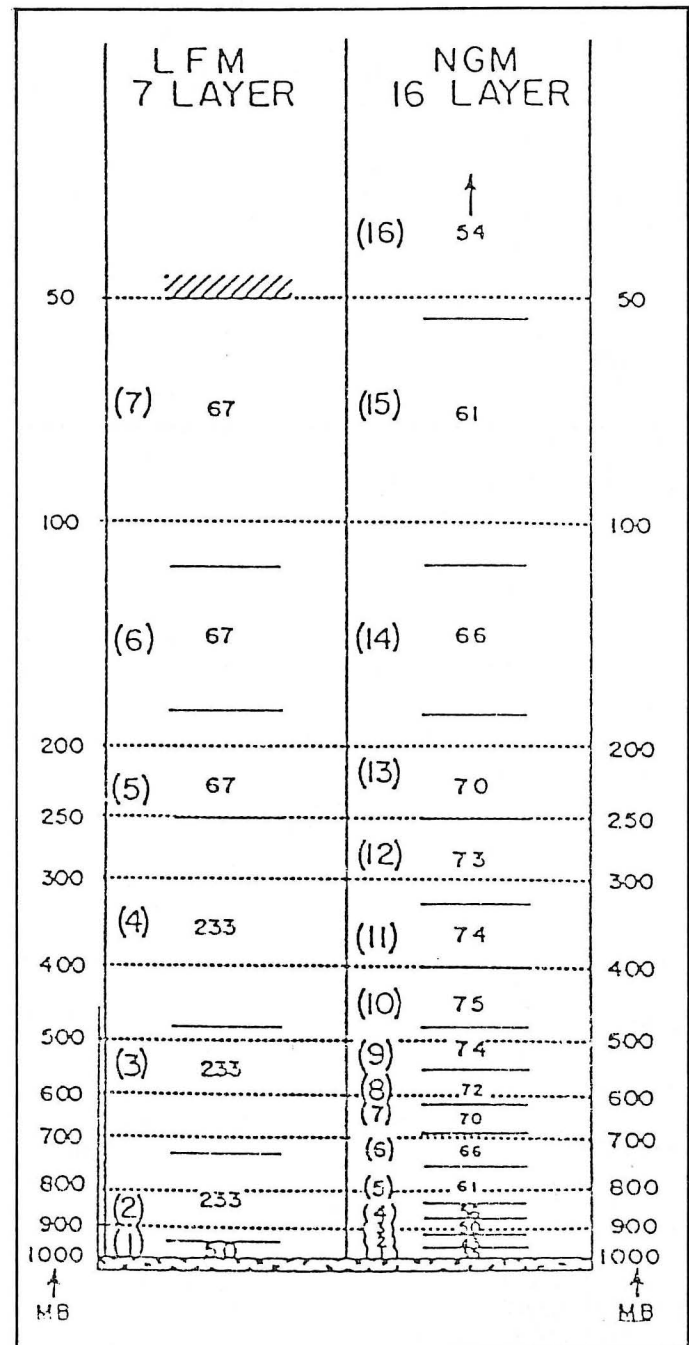


Fig. 1. Vertical structure of the NGM and LFM models. Thickness of each sigma layer is given in millibars, with the assumption that the surface pressure is 1000 mb. Note that the top of the fourth NGM layer is just below 850 mb. (Adapted from Hoke, 13).

computed by lifting parcels from each of the bottom four sigma layers dry adiabatically to saturation, then moist adiabatically to 500 mb. The difference between the parcel temperature and the predicted 500 mb temperature is calculated, with a negative value indicating instability. The most unstable value is retained; hence, the term "Four-layer Lifted Index" (4LI). Parcels in the fourth layer are just below 850 mb when the surface pressure is 1013 mb. The 4LI can at times reflect instability originating in warm air overlaying a shallow cold layer, such as in warm frontal overrunning. Note that the 4LI is similar to the Best Lifted Index documented by Fujita, *et al.* (7). The Best LI was formulated to also measure instability originating from a layer aloft since the roots of an updraft may not always originate at the surface.

It is important to discuss several differences between the SELS LI and other common stability indices, including the 4LI. The SELS LI lifts a parcel defined by the mean potential temperature and mean mixing ratio of a 100 mb thick surface-based boundary layer. (The LI computed on AFOS soundings and from the LFM model output utilize a 50 mb thick boundary layer.) The parcel is lifted to 500 mb and the parcel temperature is compared to the environmental temperature to determine the degree of instability. There are two additional aspects of the SELS LI that are unique. First, the boundary layer mean potential temperature on the 1200 GMT sounding is empirically adjusted to account for diurnal heating. The mean potential temperature of the lifted parcel is calculated by adding 2°C to the temperature at the top of the 100 mb thick boundary layer; dry-adiabatic descent of this parcel to the surface yields a simple forecast afternoon maximum surface temperature. The SELS LI computed from 1200 GMT data is more unstable than indices that do not incorporate a diurnal heating approximation. Since no additional solar heating is expected at night, the empirical adjustment is not applied to the 0000 GMT data.

Secondly, the possibility of overrunning, or elevated, instability in a layer at or below 700 mb is examined. To accomplish this, wet bulb temperatures are computed at each data level above the surface and compared with the lifted parcel temperature at that level. The level where the wet bulb temperature exceeds the parcel temperature by the largest amount, if one exists, is used as the base for a new lifted parcel. This parcel is subsequently lifted to 500 mb from the "level of overrunning." The formulation of the SELS algorithm allows detection of elevated instability that is not detected by other common indices, including the 4LI, since they do not lift parcels originating from above approximately 850 mb. Details of the automated rawinsonde analysis techniques at NSSFC are discussed by Prosser and Foster (8) and Doswell, *et al.* (9).

3. FORECAST DATA

Forecasts of the 4LI were examined during the period 15 June 1986 through 31 August 1986. Major additions to the NGM simulation of physical processes, including radiation parameterization, surface fluxes of heat and moisture, turbulent mixing, and adjustments to the convective precipitation scheme were implemented at 1200 GMT 23 July 1986. See Tuccillo and Phillips (10) for details. Note that this implementation date was at the approximate midpoint of the data sample, and provides an opportunity to study the effect of the new physics package on the 4LI forecasts.

NGM 24 and 36-h forecasts of the 4LI field were obtained from facsimile (DIFAX) maps stored at the NSSFC. For several reasons, only the 24 and 36-h predictions were examined, including:

- 1) these forecast projections provide the primary guidance for the medium-range convective outlooks (AC) issued by the Severe Local Storms (SELS) unit, and

- 2) in the early stages of a numerical forecast (0–12-h), some variables require an adjustment period to suppress computational noise and ensure that the mass and motion fields are in proper balance.

Summer outbreaks of severe thunderstorms and tornadoes tend to develop in very unstable air masses. For example, Johns and Hirt (11) have documented synoptic conditions associated with warm-season "derechos," or widespread convectively-induced windstorms. They noted that the mean SELS LI was -9°C for their sample of 70 cases. Since widespread instability is often present during the summer, the location of extreme instability is critical in the identification of potential severe weather threat areas. Although the SELS LI and the NGM 4LI are computed via different algorithms and are not strictly equivalent, they provide similar estimates of parcel buoyancy. Accordingly, the 4LI forecasts over the contiguous United States were examined for conditions of extreme instability, defined as the occurrence of areas enclosed by an isopleth value of -8 . Forecast areas on the facsimile charts that were separated by a small distance (approximately 110 km or less) were treated as one continuous area.

Table 1 presents a summary of the 4LI forecasts of extreme instability. During the study period, a total of 69 model runs produced 120 forecast areas of extreme instability. (Model output was not available for four model runs.) There was virtually no change in the relative frequency of extreme instability forecasts after the addition of the new physics package on 23 July. (Hereafter, the period from 15 June through 0000 GMT 23 July will be referred to as BP—"Before Physics," and the period beginning 1200 GMT 23 July will be AP—"After Physics.") Overall, 45% of all model runs predicted areas of extreme instability at the 24 and/or 36-h projections. When normalized per model run and projection time, there were 0.38 areas per forecast during the BP period compared to 0.42 during the AP period. Forecasts of extreme instability occurred more frequently in model runs based upon 0000 GMT initial data. This tendency became more pronounced in the AP period (Table 2). Finally, Table 3 reveals there is no significant bias toward projection times (24 or 36-h) or valid times (0000 or 1200 GMT), although the percentage of forecast areas valid at 0000 GMT and on the 36-h projection increased slightly in the AP period.

Table 1. Summary of NGM Forecasts of Extreme Instability (EI)

	Number of EI Forecast Areas	Number of Model Runs Fcstg EI	Total Model Runs in Data Sample	% of Model Runs Fcstg EI
BP Period	55	33	73	45
AP Period	65	36	79	46
Totals	120	69	152	45

Table 2. Initial Data Time of NGM Forecasts of Extreme Instability (EI). Numbers in Parentheses Refer to the Percent of Areas or Model Runs During the Data Period.

	Number of EI Forecast Areas	Number of Model Runs Forecasting EI
BP Period		
1200 GMT	22 (40)	13 (39)
0000 GMT	33 (60)	20 (61)
AP Period		
1200 GMT	23 (35)	12 (33)
0000 GMT	42 (65)	24 (67)

Table 3. Forecast Projection and Valid Time of NGM Predictions of Extreme Instability Areas

	Forecast Projection		Forecast Valid Time (GMT)	
	24-h	36-h	1200	0000
BP Period	30	25	29	26
AP Period	33	32	29	36

4. VERIFICATION OF FORECASTS

To determine the accuracy of the 4LI forecasts of extreme instability, the 120 cases were compared with the NGM 4LI 00-h forecast valid at the verifying times. The 00-h forecast in the NGM consists of data interpolation to sigma coordinates followed by a Normal Mode Initialization (NMI) to suppress noise. Additional interpolation back to pressure coordinates is then accomplished. The NGM 00-h forecast is not equivalent an "initial analysis" owing to the NMI procedure and the coordinate transformation.

a) Forecast Assessment

A detailed verification of grid point data is beyond the scope of this study. However, it was possible to evaluate a range of predicted 4LI values based upon the contour interval on the facsimile charts. To accomplish this, each range of 4LI values was assigned a categorical designator:

- CAT 1 : +4 to 0
- CAT 2 : 0 to -4
- CAT 3 : -4 to -8
- CAT 4 : -8 to -12
- CAT 5 : -12 to -16

Any area enclosed by the predicted -8 contour was manually transferred onto the appropriate 00-h initial conditions, and a categorical verification of each individual forecast area was performed. This aspect of the verification is equivalent to the determination of a False Alarm Ratio, since it examines the number of correct versus incorrect forecast areas of extreme instability. For example, if a CAT 4 (-8 to -12) forecast area verified within the CAT 3 (-4 to -8) contour, the prediction was an overforecast of one category. (That is, $CAT_{\text{fcst}} - CAT_{\text{verf}} = \text{error}$, with positive errors indicating an overforecast. An overforecast error means that more instability was forecast than actually occurred.) This verification method effectively smooths any small scale variations in the 4LI fields during the error analysis. Further, this method accentuates the relative degree of instability that is commonly used in convective forecasting rather than focusing on specific values (Miller, 2).

In most cases, the error analysis was straightforward, with forecast areas generally located completely within one verification category. For cases where the forecast area straddled two or more verifying categories, one category was selected if it covered at least two thirds of the forecast area. If this were not applicable, an average of the possible verifying categories was used. This averaging method was required in only a small number of cases. Some sample forecasts and verifying conditions are shown in Figs. 2 and 3. In these cases, the NGM incorrectly forecast the occurrence of extreme instability from Illinois into southwest Lower Michigan (Fig. 2), and over parts of the Carolinas (Fig. 3). Note also in Fig. 3 that the 00-h extreme instability observed over parts of the Dakotas and northwest Minnesota was underforecast by the preceding 24-h prediction.

Mean forecast errors are presented in Table 4. Overall, only 5% of the forecasts verified in the proper category. All six correct forecasts occurred during the AP period, and one half of these originated from initial instabilities of -8 or less over the forecast area. In the other cases (95% of the sample) of predicted extreme

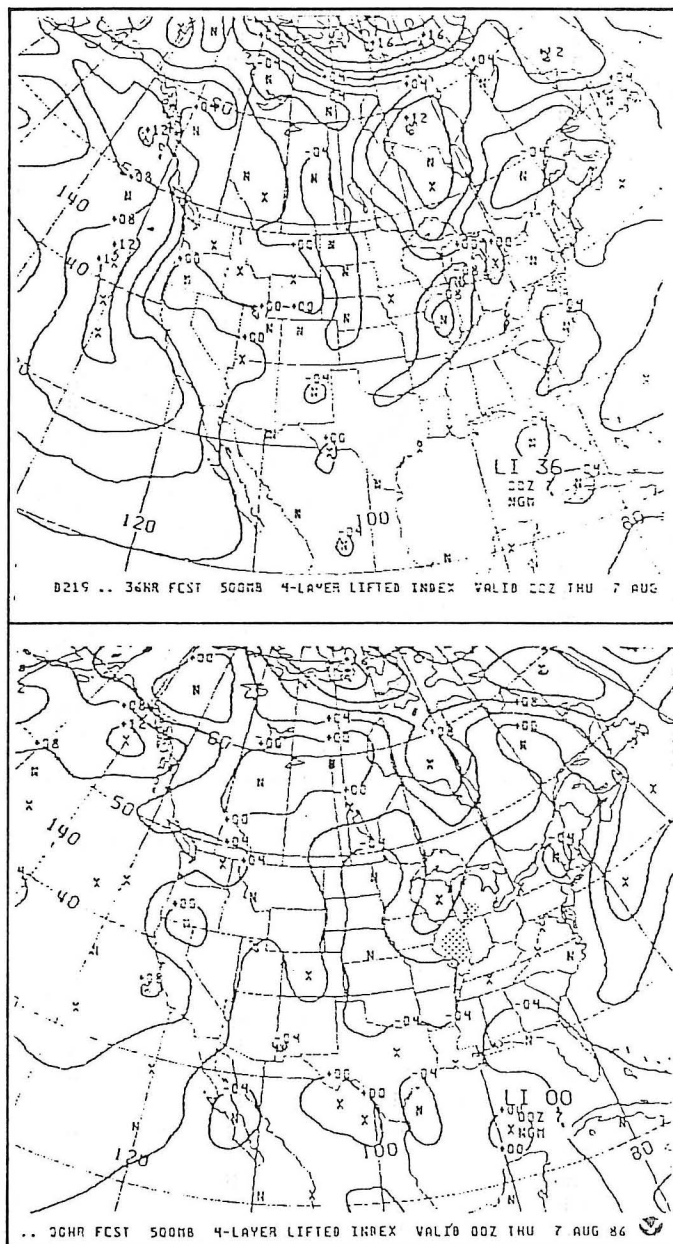


Fig. 2. NGM four-layer lifted index 36-h forecast valid 0000 GMT 7 August 1986 (top) and 00-h verifying conditions (bottom). Note forecast of extreme instability from Illinois into southwest lower Michigan, which is denoted by stippling on the 00-h verifying chart.

instability, the destabilization process was overforecast, particularly during the AP period.

While the mean statistics provide useful information, it is also informative to examine frequency distributions of categorical forecast errors. Fig. 4 reveals an overall shift toward larger errors during the AP period. Large errors, defined as errors of two categories or more, occurred in more than two thirds (71%) of the cases during the AP period, whereas less than 40% of the errors during the BP period were large. Note that more than 10% of the AP cases contained errors of three categories or more. In most instances, forecast errors were not simply one of either location (e.g., the forecast instability category was correct, but the location needed minor adjustment), or one of magnitude (e.g., the axis of maximum instability was correctly located, but the degree of instability was underforecast). Rather, most errors consisted of combinations of both location and magnitude.

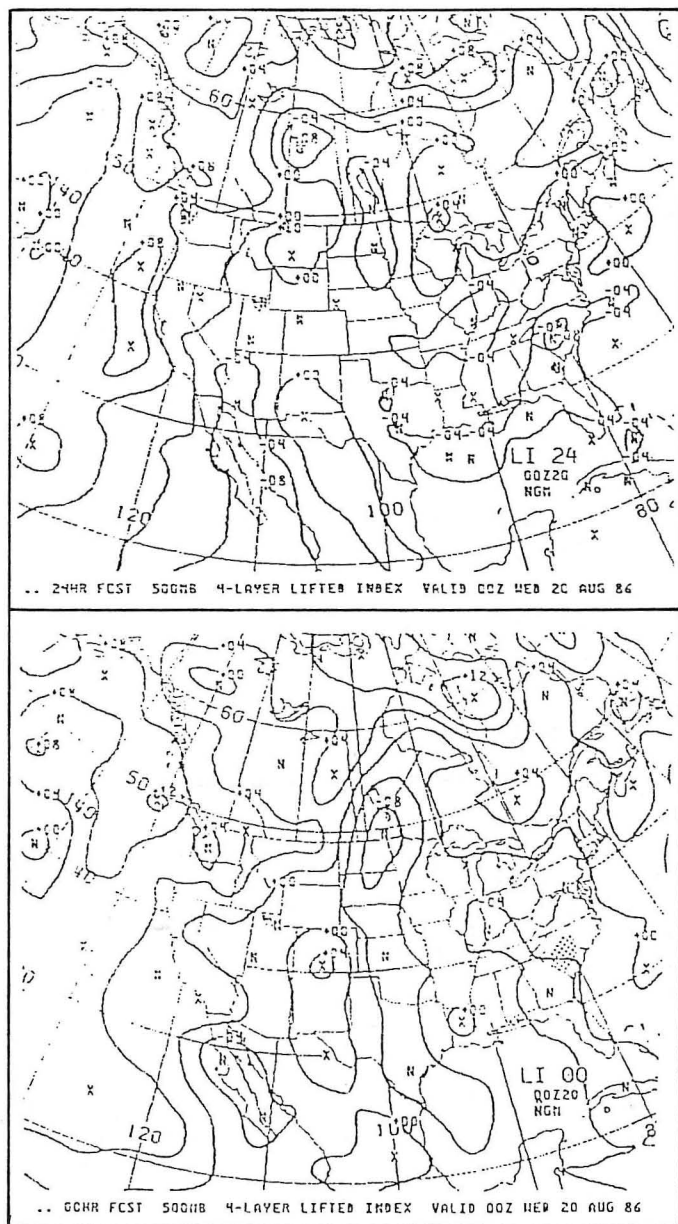


Fig. 3. As in Fig. 2, except 24-h forecast valid 0000 GMT 20 August 1986. Note forecast of extreme instability across the Carolinas.

b) Quality of Verifying Data

To ensure that the small number of correct forecasts of extreme instability was not a reflection of unrepresentative verifying conditions, the initial fields of the 4LI were examined in more detail. It is possible that the 00-h extreme instability could be underestimated because of the large distance (~400 km) between rawinsonde stations. This possibility was exacerbated by the

high frequency of missing rawinsonde data during the summer of 1986. On the other hand, surface data, including temperature and moisture, are incorporated into the NGM analysis procedure. It is also plausible that some aspects of the 00-h 4LI field are actually a reflection of the higher resolution surface data, especially since some areas of 00-h extreme instability were located between rawinsonde sites. This is analogous to the computation of a surface-based LI field where much of the detail is supplied by the surface observation network (Hales and Doswell, 12). However, unlike the direct methodology of the surface-based LI computation, the surface data utilized by the NGM are adjusted by the model initialization procedure; see Hoke (13) for details. It is not clear how the NGM pre-processing scheme ultimately affects the delineation of instability. Thus, the accuracy of the 00-h stability fields cannot be totally evaluated owing to the coarse upper air data resolution and limitations in current remote sensing systems such as VAS derived soundings (Mostek, *et. al.*, 14).

All 0000 GMT cases were subjectively compared with computations of the SELS LI to ascertain how well the 00-h model forecast simulated observed atmospheric conditions. (Recall that the 1200 GMT SELS LI is not directly comparable to other stability indices since the algorithm contains a diurnal heating approximation.) The comparison indicated surprisingly good reliability of the 00-h fields, especially since the algorithms used to calculate the two indices are not equivalent. See Fig. 5 for a sample comparison.

As seen in Table 5, the model initialized areas of extreme instability on more than 28% of its runs during the sampling period. The relative frequency of occurrence was slightly higher during the BP period. When the frequency of occurrence of 00-h extreme instability was normalized, there were 0.38 areas per model run during the BP period, compared to 0.29 areas during AP. Note that the BP frequency of occurrence of 0.38 was identical to the frequency of prediction discussed in section 3. During the AP period, however, the frequency of prediction (0.42) was greater than the frequency of occurrence (0.29), implying a tendency to overforecast the occurrence of extreme instability. Nearly two thirds of the initial conditions of extreme instability occurred at 0000 GMT (Table 6). These results are consistent with the idea that there is greater instability from spring through early summer, and greater instability during the late afternoon hours than during the morning.

The ability of the NGM to predict extreme instability when it did occur was also examined. Forecasts at the 24 and 36-h projections were compared to actual conditions of extreme instability that were identified on the 00-h forecasts. This is equivalent to the determination of a Probability of Detection. Table 7 indicates that conditions of extreme instability were usually underforecast, with larger errors occurring at the 36-h projection. The distribution of categorical errors is shown in Fig. 6. The error frequency displayed a tendency to shift somewhat toward smaller underforecast errors during the AP period. Also, large underforecast errors (defined as errors of two categories or more) of actual conditions of extreme instability occurred in 51% of the BP cases, but were less frequent during the AP period. A comparison of the mean errors (taken from Tables 4 and 7 and shown in Fig. 7) suggests that the NGM forecasts of the 4LI became

Table 4. Mean Categorical Errors for NGM Forecasts of Extreme Instability. Times in GMT.

	Projection Time		Valid Time		All Cases	Correct Forecasts	Total Forecasts
	24-h	36-h	0000	1200			
BP Period	1.37	1.42	1.38	1.39	1.39	0	55
AP Period	1.61	1.84	1.67	1.79	1.72	6	65

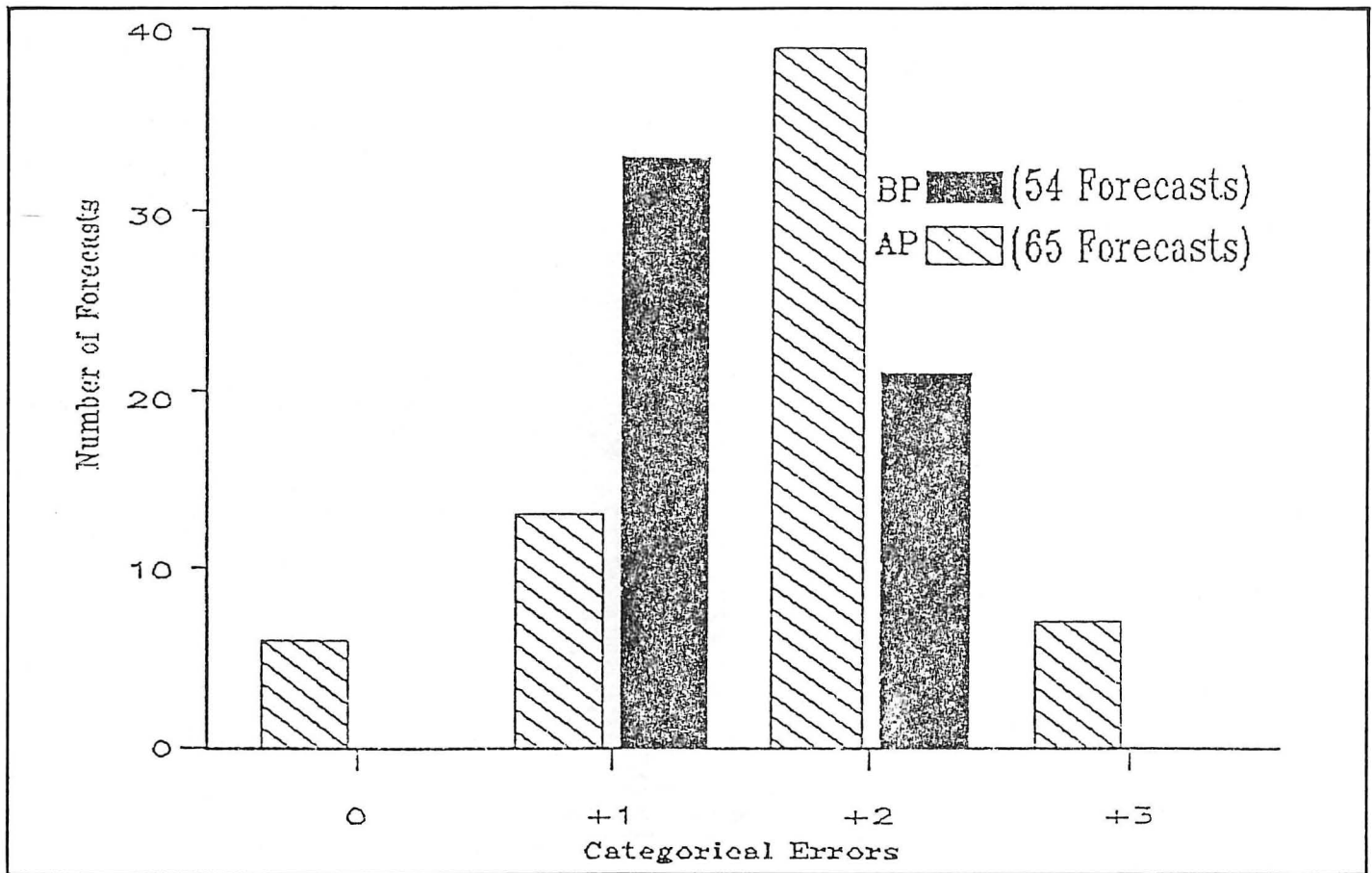


Fig. 4. Distribution of categorical errors for all NGM four-layer lifted index forecasts of extreme instability (24 and 36-h predictions combined) during BP period (solid) and AP period (hatched). Positive errors indicate an overforecast.

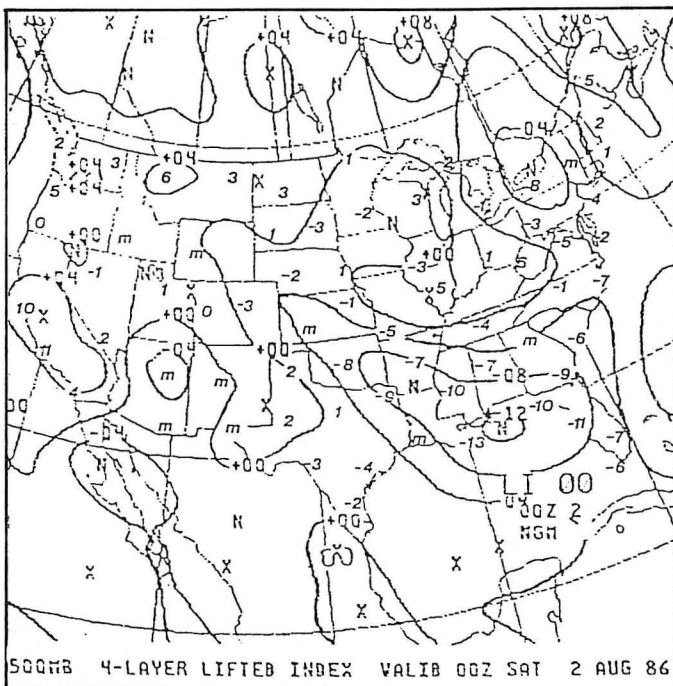


Fig. 5. NGM four-layer lifted index 00-h initial conditions for 0000 GMT 2 August 1986 denoted by contoured analysis. SELS Lifted Index values superimposed at location of rawinsonde stations. Missing rawinsonde data indicated by the letter "m".

Table 5. Summary of NGM 00-h Conditions of Extreme Instability (EI)

	Number of Areas of 00-h EI	Number of Model Runs With 00-h EI	Total Model Runs in Sample	% of Model Runs with 00-h EI
BP Period	28	23	73	32
AP Period	23	20	79	25
Totals	51	43	152	28

Table 6. Time of NGM 00-h Conditions for Areas of Extreme Instability

	1200 GMT	%	0000 GMT	%
BP Period	11	39	17	61
AP Period	7	30	16	70
Totals	18	35	33	65

Table 7. Mean Categorical Errors for NGM Forecasts Valid at 00-h Conditions of Extreme Instability

	Projection Time		All Cases	Correct Forecasts	Total Forecasts
	24-h	36-h			
BP Period	-1.50	-1.75	-1.63	1	55
AP Period	-1.28	-1.43	-1.36	1	46

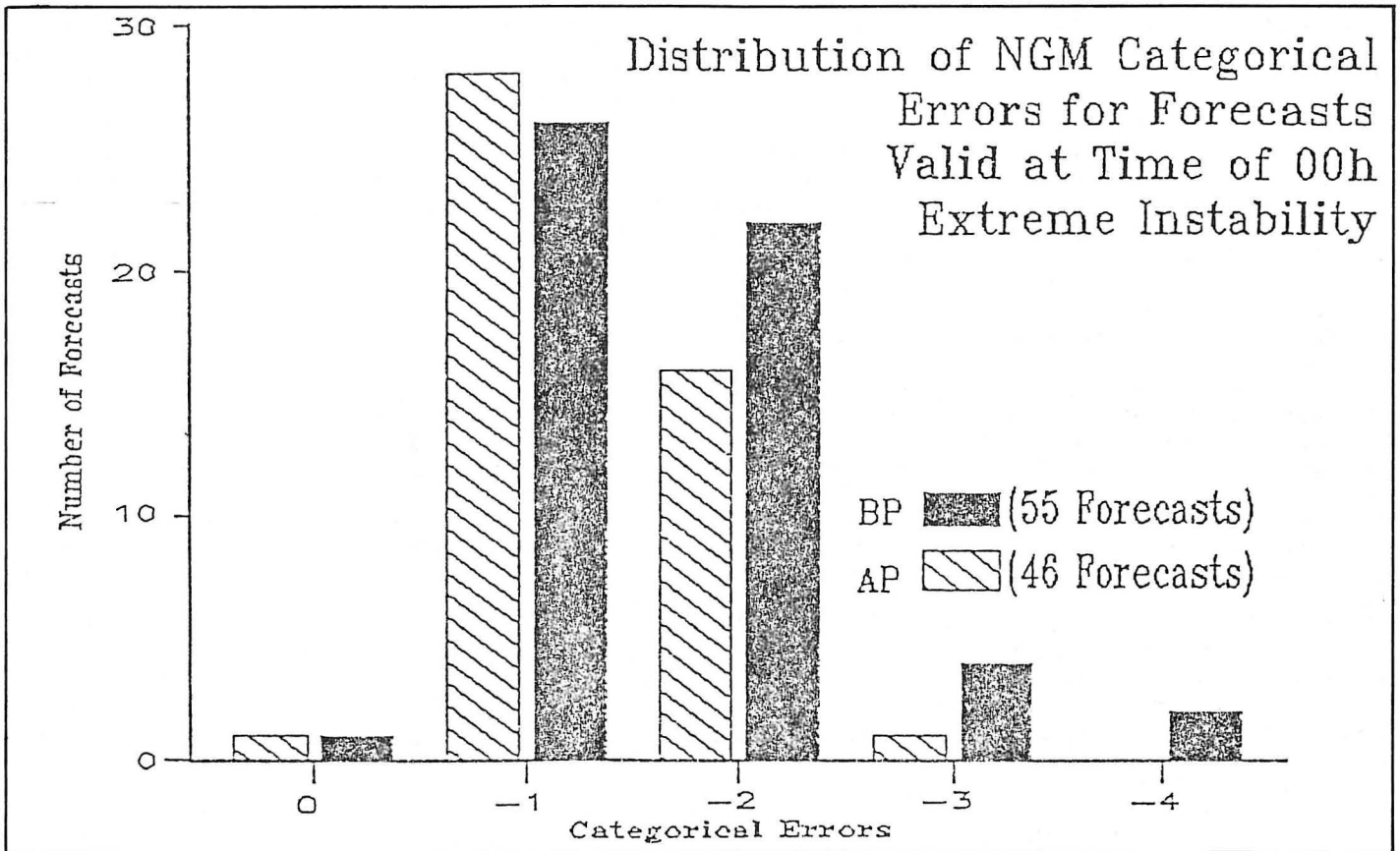


Fig. 6. As in Fig. 4, except all forecasts valid at the time of 00-h extreme instability. Negative errors indicate an underforecast.

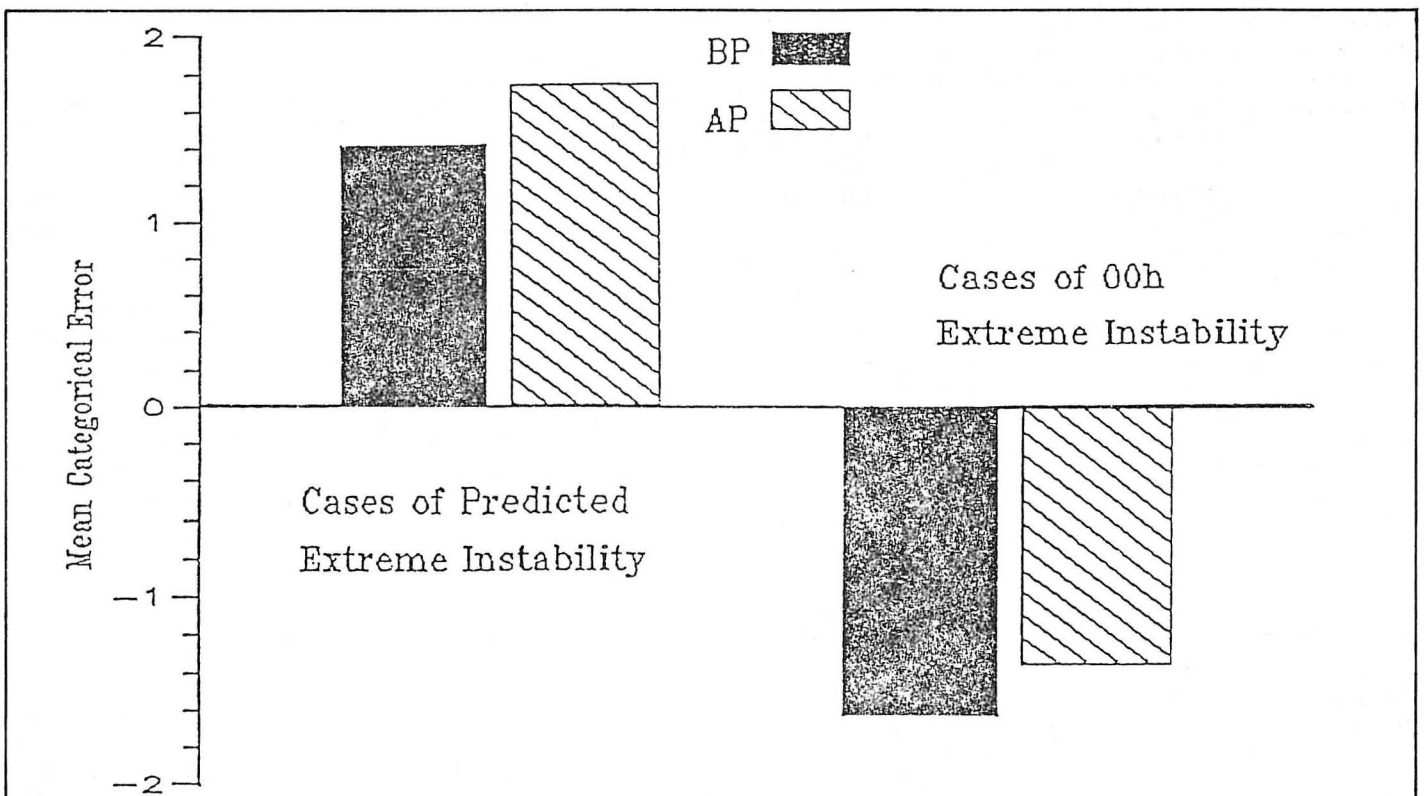


Fig. 7. Mean categorical errors for NGM four-layer lifted index 24 and 36-h forecasts of extreme instability (left), and for 24 and 36-h forecasts valid at the time of 00-h extreme instability (right). Hatching refers to AP period and solid refers to BP period. Positive (negative) errors indicate an overforecast (underforecast). See text for details.

more unstable (in a relative sense) during the AP period, since the vertical coordinate in Fig. 7 is roughly proportional to the amount of instability.

c) Relationship to Forecast Precipitation

A key consideration in the introduction of the more complete physical processes in the NGM was the desire to improve warm season precipitation forecasts. Test results during June 1986 indicated a major improvement in precipitation threat scores for the revised NGM (Tuccillo and Phillips, 10). In this study, the relationship between forecast precipitation and large errors in the forecast of extreme instability by the 4LI was examined, since the large error situations potentially have the most serious impact on the operational forecaster. The large error cases identified in section 4a were screened for the occurrence of the following forecast parameters: 1) measurable precipitation, and 2) a printed precipitation maximum (QPF_{max}), located within or very close to the area of predicted extreme instability. The QPF_{max} were also examined for the appearance of localized excessive amounts, or "bulls-eyes," defined as quasi-circular areas of maximum precipitation consisting of two or more concentric isohyets (contour interval of 0.5 inches on the facsimile charts).

Table 8 indicates that a marked change in the model precipitation efficiency occurred in the AP period, when all large instability error cases were associated with measurable precipitation. Further, nearly three quarters of the large error AP cases had a QPF_{max} located within or very close to the extreme instability forecast area, and almost one third of the large error AP cases were associated with QPF_{max} bulls-eyes. In dramatic comparison, only a small percentage of the BP large error cases had any forecast precipitation near the predicted location of extreme instability.

Table 8. Summary of Large Categorical Forecast Errors of NGM Forecasts of Extreme Instability and Associated Forecast Precipitation. Numbers in Parentheses Refer to Percent of Cases During Period.

	Cases with Measurable Precipitation	Cases with QPF_{max}	Cases with QPF_{max} Bulls-eye
BP Period	4 (19)	3 (14)	2 (10)
AP Period	46 (100)	33 (72)	14 (30)

The distribution of forecast QPF_{max} and precipitation bulls-eye amounts (Table 9) reveals that nearly three quarters of the QPF_{max} amounts associated with large forecast errors of extreme instability during the AP period consisted of 12-h accumulations of 1.0 inch or greater, and that the majority of bulls-eye cases predicted at least 2.0 inches of rain. Finally, all extreme instability forecast areas that were virtually coincident with QPF_{max} bulls-eye cases were associated with large overforecasts of instability.

Table 9. Distribution of NGM Forecasts of 12-h Accumulated Precipitation for Large Error Cases During the AP Period

12-h Accumulated Precipitation (in)	Number of Cases with QPF_{max}	Number of Cases with Bulls-eyes
<0.50	2	0
0.50-0.99	7	0
1.00-1.49	10	3
1.50-1.99	6	3
≥2.00	8	8

5. DISCUSSION

This analysis indicates that the NGM model has difficulty in forecasting conditions of extreme instability during the warm season. The 24 and 36-h projections of extreme instability typically overforecast the degree of instability, and this tendency has become more pronounced since the implementation of the revised physics package on 23 July 1986. A thorough analysis of the problem can only be accomplished by sensitivity tests on the model and is beyond the intent of this study. However, sufficient documentation of the NGM physical processes is available to allow speculation on possible causes of the increase in the extreme instability forecast errors.

An air column can destabilize by several basic processes:

1. Cooling and/or drying of the upper layers
2. Heating and/or moistening of the lower layers

Any combination of 1 and 2 acting in concert will act to decrease the stability of the column. Specific atmospheric mechanisms known to contribute to destabilization include differential horizontal advection and upward vertical motion. Differential horizontal advection, described by Miller (15) and McNulty (16), is associated with vertical differences in the horizontal advection of heat and moisture. Doswell (3) points out that differential horizontal advection can increase the lapse rate of a sounding by as much as $1^{\circ}\text{C km}^{-1}$ every three hours. Secondly, synoptic scale ascent is also a major influence on the stability. As documented by Hess (17), the lifting of a layer always destabilizes a stable layer, with the lapse rate becoming more nearly dry adiabatic. Further, upward vertical motion can also result in the elimination of a low-level inversion which typically inhibits convective development in a pre-storm environment (Beebe and Bates, 18). Thus, while differential horizontal advection can contribute to the formation of an unstable air mass, upward vertical motion contributes to both the formation and release of the instability (House, 19; Newton, 20).

Accordingly, it is possible to infer changes in stability by identifying possible thermodynamic effects of the physical processes simulated in the NGM. Phillips (21) recently identified and corrected a problem with the vertical mixing of heat and moisture that occurred rather infrequently. When this error occurred it apparently affected only a small number of grid points, thus contributing to a localized large error in the 4LI calculation. The case cited by Phillips (21) also involved the generation of consecutive QPF_{max} bulls-eyes with maximum amounts greater than three inches. The number of forecasts in the current data sample similar to this case is relatively small. Further, the appearance of large overforecasts of extreme instability has continued after the correction was implemented. Thus, it is hypothesized that other aspects of the revised physics have also contributed to the instability forecast errors. These include:

A. Kuo Convective Precipitation Procedure

1. The moist convective adjustment was altered to allow more efficient condensation of moisture accumulated due to advection, etc. If the enhanced latent heat release occurs in any of the bottom four model layers, an increase in the lapse rate is a possible result.

2. The saturation criterion that allows convective condensate to fall through a layer (rather than evaporate) was lowered from about 95% to 50%. This change makes it much easier for convective precipitation to reach the ground. However, less evaporational cooling will also occur as the precipitation falls. Heuristically one would expect a net warming of the lower layers relative to the previous formulation. However, the situation is very complicated, and additional effects on the vertical heating profile occur when the saturation criterion is lowered. Thermodynamic computations and numerical model experiments by Mathur (22) indicated that marked cooling occurred in the middle

and upper troposphere when the criterion was reduced from 100% to 80%. In his study, the cooling aloft caused by the vertical advection and subsequent evaporation of moisture apparently was larger than the heating generated by large-scale release of latent heat, and resulted in the temperature lapse rate becoming more unstable.

The convective adjustment scheme in the NGM is performed at each model grid point having 1) sufficiently large low-level moisture convergence, and 2) a buoyant cloud profile originating from one of the lowest four model layers. A *subgrid-scale* Kuo-type parameterization (Rosenthal, 23; Frank, 24) is used in the NGM to limit the unstable growth of disturbances when saturation develops under convectively unstable conditions. For meso- α scale models (grid spacing 50–250 km), such as the NGM, cumulus parameterization schemes can adequately simulate convective condensation, transports of heat, moisture and momentum, and the interaction of the cumulus cloud with the large-scale environment (Molinari and Dudek, 25). However, such parameterization solutions are quite sensitive to factors such as precipitation efficiency, entrainment and the resultant partitioning of available latent heat energy into moistening and heating processes. Therefore, it is not uncommon for parameterization schemes to predict convective heating profiles with a level of maximum heating lower than the observed one (Kuo and Anthes, 26). This can result in excessive convective instability as indicated by Molinari (27).

It is hypothesized that the occasional appearance of excessively low surface pressures and localized heavy precipitation in the NGM output (Hirt, 28) may arise from difficulties with the convective adjustment scheme. Apparently, the excessive liberation of latent heat in the lower troposphere can lead to surface pressure falls, enhanced upward motion and additional condensational heating. It is noteworthy that a similar positive feedback process also occurred in a mesoscale model that did not incorporate a cumulus parameterization scheme (Koch, *et al.*, 29). Other experiments by Molinari and Dudek (25) which included only grid-scale convective processes also produced excessive convective instability and the unstable growth of rainfall, even when the saturation criterion was reduced.

These results illustrate the difficulty in properly simulating the effects of convection in numerical models, and make it apparent that no consensus exists on how to best incorporate cumulus convection into mesoscale models.

B. Diurnal Heating Cycle

Figure 8 shows the mean 12-h temperature error in the lowest model layer for forecasts verifying at 0000 GMT. The large errors in California are attributed to terrain variation and inadequate sampling by rawinsondes. However, a large overforecast of the boundary layer temperature is also present over much of the Mississippi Valley region. It is unlikely that this error is caused by terrain problems. If the diurnal cycle tends to warm the boundary layer too much, excessive destabilization of the column will occur. However, according to Table 4, the mean overforecast error during the AP period was slightly larger for the 4LI predictions verifying at 1200 GMT. This occurred even though a *negative* 12-h mean temperature error was present in the NGM bottom layer at this time (Fig. 9). This suggests that the model bottom layer temperature errors may not be a significant source of the instability overforecast errors. The nature of the unstable growth in the NGM may differ from that reported by Molinari and Dudek (25), who concluded that the presence of diurnal warming was an essential contributor to the excessive prediction of rainfall.

C. Mid-tropospheric Height and Temperature Forecasts

An error analysis of the 48-h NGM 500 mb height forecasts (Fig. 10) indicates that the negative height anomalies have

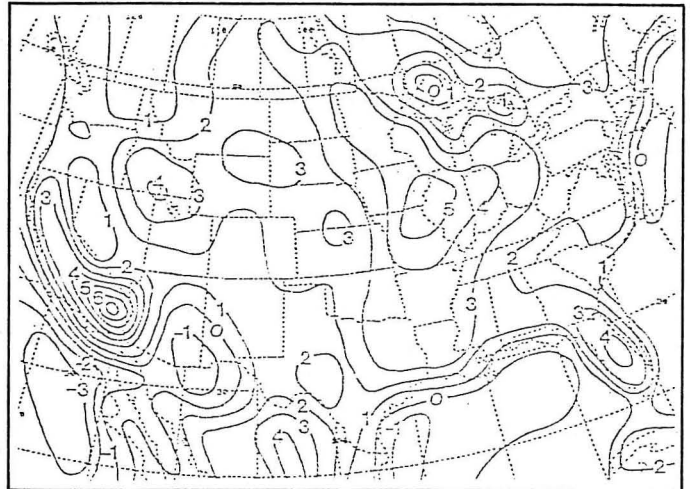


Fig. 8. NGM mean temperature error ($^{\circ}\text{C}$) in lowest sigma layer for 12-h forecasts verifying at 0000 GMT, for the period from 9 June through 3 July 1986. (From Tuccillo and Phillips, 10).

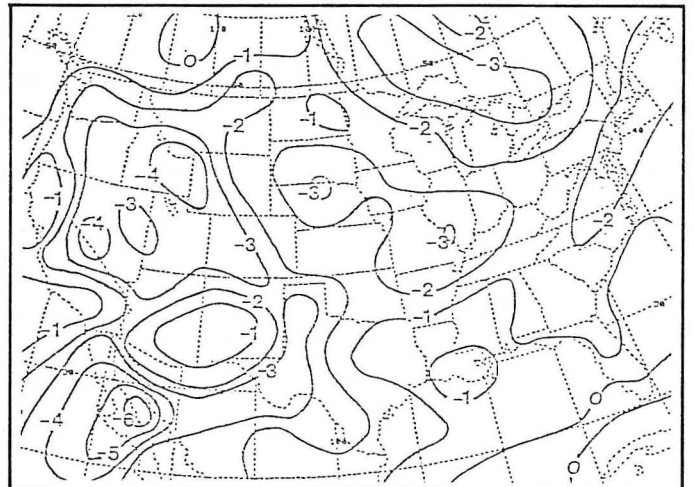


Fig. 9. As in Fig. 8, except verifying at 1200 GMT. (From Tuccillo and Phillips, 10).

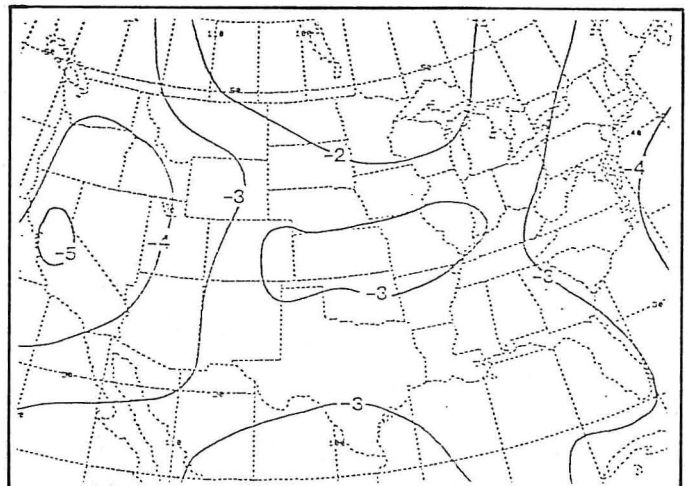


Fig. 10. NGM mean 500 mb height error (decameters) for all 48-h forecasts during the period from 9 June through 30 June 1986. (From Tuccillo and Phillips, 10).

increased during the AP period (Tuccillo and Phillips, 10). Mean height errors of at least 30 meters, which are equivalent to nearly 1°C, cover much of the nation. This is in agreement with other reports (Phillips, 30) which have discussed a continuing cold bias in the NGM middle troposphere (Fig. 11). Since the cold bias is also present at earlier forecast projections, a steepening of the lapse rate will result not only at the 48-h projection, but at the 24 and 36-h forecast as well. The reason for the systematic cold bias has not been determined.

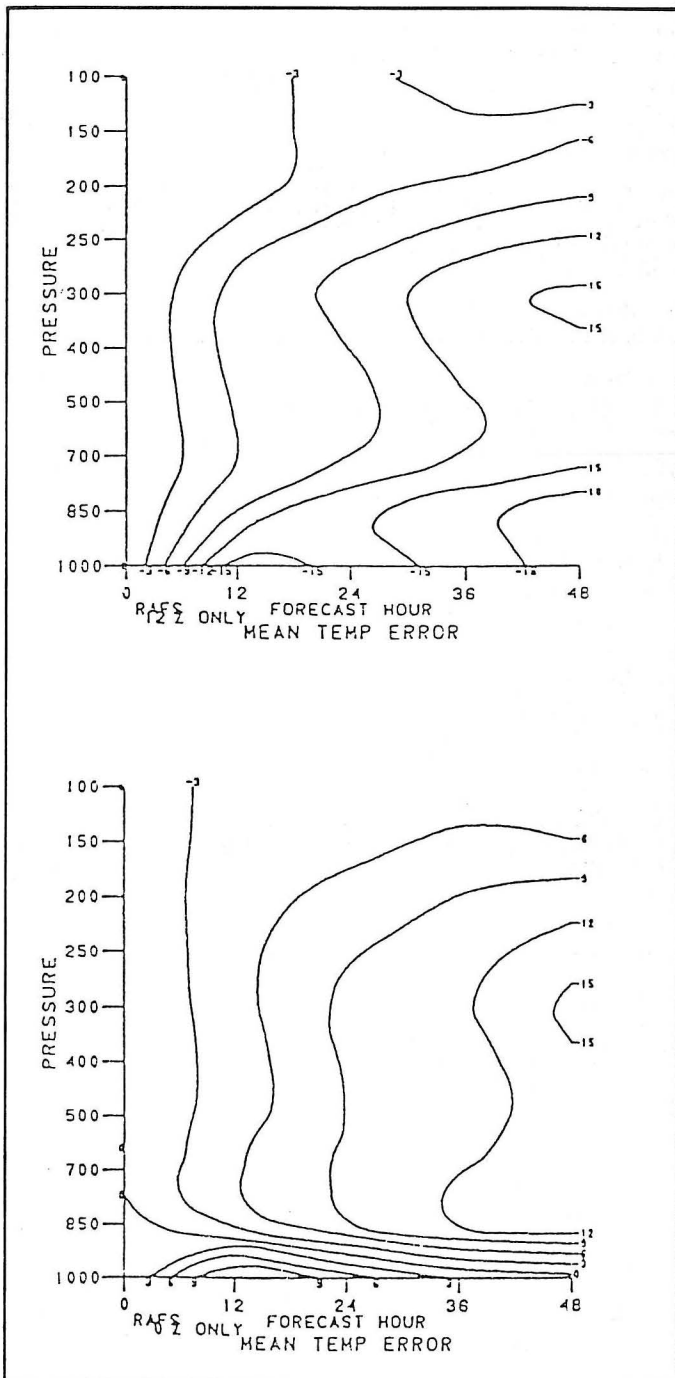


Fig. 11. NGM mean temperature error (0.1°C) for all 1200 GMT model runs (top) and for all 0000 GMT model runs (bottom) averaged over the North American continent during September, 1986. According to Phillips (30), values below 850 mb should be ignored.

D. Evaporation of Soil Moisture

The computation of the surface energy budget requires the specification of moisture availability (MA). The MA is derived from climatological data and is subject to great uncertainty. Excessive evaporation of soil moisture will contribute to additional moisture in the lowest model layers and can enhance the destabilization of the column. Sensitivity experiments by Diak, *et al.* (31) examined the effect of variations in surface parameters on mesoscale model forecasts. In particular, an increase in the MA resulted in an increase in both latent heat and total precipitation. They also reported that, especially in dry regions, small errors in the assessment of the MA caused very large errors in surface temperature and the surface heat balance. Ookouchi, *et al.* (32) noted that horizontal discontinuities in the MA can induce significant variation in surface thermal forcing and that important mesoscale circulations result from variations in soil moisture. In addition, Benjamin (33) has shown that the development of an elevated mixed layer inversion typical in a pre-storm environment is strongly influenced by the presence of an upstream MA gradient. Thus, it appears that accurate specification of the MA is needed to properly represent many mesoscale features of operational significance (Kaplan, *et al.*, 34).

While comparison with other simulation experiments can provide insight into the possible cause of the model errors, any comparison must be viewed with some caution since different numerical models do not treat all physical processes alike. Thus, insight gained from one model may not be totally applicable to another model. It is difficult to accurately assess the impact of various effects on the 4LI computations. However, based primarily on subjective examination of the data sample and the close relationship between the predicted warm season precipitation and the 4LI forecasts, it is hypothesized that the convective adjustment scheme may be a major contributor to the 4LI errors.

6. CONCLUSIONS

To aid operational forecasters, NGM forecasts of air mass stability were examined for the period from 15 June through 31 August 1986. The following conclusions may be helpful when utilizing NGM predictions of extreme instability (defined as areas enclosed by the -8 4LI isopleth):

- Predictions of extreme instability were nearly always overforecast.
- The magnitude of the overforecast errors increased after the revised physics package was implemented in July 1986 (the AP period). Nearly three quarters of the AP predictions overforecast the instability by 8°C or more.
- When conditions of extreme instability actually occurred, the NGM tended to underforecast the instability.
- The magnitude of the underforecast errors diminished during the AP period. Approximately one third of the AP predictions underforecast the instability by 8°C or more.
- Unlike the BP period, when a dry bias was evident, forecasts of extreme instability during the AP period were usually accompanied by forecasts of measurable precipitation.
- Large overforecast errors during the AP period were often coincident with forecast precipitation maxima, and were occasionally associated with precipitation bulls-eyes.
- Forecasts of extreme instability that were coincident with a precipitation bulls-eye were always associated with large overforecasting errors.

In summary, the NGM forecasts of extreme instability have a very high False Alarm Ratio and a very low Probability of Detection. Although this study examined only warm season data, operational experience indicates that the 4LI performance

characteristics listed above are applicable during the cool season as well. It is important to realize, however, that the results of this research cannot be used to evaluate the overall utility of the 4LI predictions. This study did not address other aspects of the 4LI performance, such as whether skill exists in the prediction of stability trends, systematic errors in the forecast location of unstable centers, the geographic distribution of errors, and the relationship between synoptic patterns and prediction errors. Additional research into these areas utilizing a grid point data analysis technique would provide beneficial information for both research and operational meteorologists regarding the overall reliability of the NGM 4LI predictions.

7. ACKNOWLEDGEMENTS

I would like to thank Dr. Joseph Schaefer (National Weather Service, Central Region) and Dr. Norman Phillips (National Meteorological Center) for their many suggestions for improving the manuscript. Additional review was provided by Messrs. Frederick Ostby and William Hirt (NSSF) and Dr. James Moore (St. Louis University). Discussions with Drs. James Hoke, Geoffrey DiMego and James Tuccillo (NMC) were very helpful in clarifying aspects of the NGM initialization and precipitation procedures. Mr. William Hirt also produced the graphs utilized in the study.

NOTES AND REFERENCES

1. Steven J. Weiss is a Lead Severe Local Storms (SELS) forecaster at the National Severe Storms Forecast Center. Previous assignments include duty at the National Weather Service Forecast Offices at Chicago and Detroit, and at the National Severe Storms Laboratory in Norman, Oklahoma. His meteorology degrees were received from the University of Oklahoma (B.S.) and the University of California at Los Angeles (M.S.).
2. Miller, R.C., 1972: Notes on analysis and severe-storm forecasting procedures of the Air Force Global Weather Central. AWS TR 200 (Rev.), Hdqtrs. Air Weather Service, Scott AFB, IL.
3. Doswell, C.A., III, 1982: The operational meteorology of convective weather. Volume 1: operational mesoanalysis. NOAA Tech. Memo., NWS NSSFC-5, Kansas City, MO.
4. McNulty, R.P. 1985: A conceptual approach to thunderstorm forecasting. Nat. Wea. Digest, 10, 26-30.
5. Showalter, A.K., 1953: A stability index for thunderstorm forecasting. Bull. Amer. Meteor. Soc., 34, 250-252.
6. Galway, J.G., 1956: The lifted index as a predictor of latent instability. Bull. Amer. Meteor. Soc., 37, 528-529.
7. Fujita, T.T., D.L. Bradbury and C.F. Van Thullenar, 1970: Palm Sunday tornadoes of April 11, 1965. Mon. Wea. Rev., 98, 29-69.
8. Prosser, N.E. and D.S. Foster, 1966: Upper air sounding analysis by use of an electronic computer. J. Appl. Meteor., 5, 296-300.
9. Doswell, C.A., III, J.T. Schaefer, D.W. McCann, T.W. Schlatter and H.B. Wobus, 1982: Thermodynamic analysis procedures at the National Severe Storms Forecast Center. Preprints, Ninth Conference on Weather Forecasting and Analysis, Amer. Meteor. Soc., Seattle, 304-309.
10. Tuccillo, J.J. and N.A. Phillips, 1986: Modeling of physical processes in the Nested Grid Model. Tech. Proc. Bull. 363, National Meteorological Center, National Weather Service, Silver Spring, MD, 24 pp.
11. Johns, R.H. and W.D. Hirt, 1987: Derechos . . . widespread convectively-induced windstorms. (Accepted for publication in Weather and Forecasting)
12. Hales, J.E. and C.A. Doswell, III, 1982: High resolution diagnosis of instability using hourly surface lifted parcel temperatures. Preprints, Twelfth Conference of Severe Local Storms, Amer. Meteor. Soc., San Antonio, 172-175.
13. Hoke, J.E., 1984: Forecast results for NMC's new regional analysis and forecast system. Preprints, Tenth Conference on Weather Forecasting and Analysis, Amer. Meteor. Soc., Clearwater Beach, 418-423.
14. Mostek, A., L.W. Uccellini, R.A. Petersen and D. Chesters, 1986: Assessment of VAS soundings in the analysis of a preconvective environment. Mon. Wea. Rev., 114, 62-87.
15. Miller, J.E., 1955: Intensification of precipitation by differential advection. J. Meteor., 12, 472-477.
16. McNulty, R.P., 1980: Differential advection of wet-bulb potential temperature and convective development: An evaluation. Preprints, Eighth Conference on Weather Forecasting and Analysis, Amer. Meteor. Soc., Denver, 286-291.
17. Hess, S.L., 1959: Introduction to Theoretical Meteorology. Holt, Rinehart and Winston, New York, 362 pp.
18. Beebe, R.G. and F.C. Bates, 1955: A mechanism for assisting in the release of convective instability. Mon. Wea. Rev., 83, 1-10.
19. House, D.C., 1958: Air mass modification and upper level divergence. Bull. Amer. Meteor. Soc., 39, 137-143.
20. Newton, C.W., 1963: Dynamics of severe convective storms. Meteor. Monograph, 5, Severe Local Storms, Amer. Meteor. Soc., Boston, 33-58.
21. Phillips, N.A., 1986a: Correction to vertical mixing in the NGM forecast code. Western Region Tech. Attachment 86-27, National Weather Service, Salt Lake City, UT, 4 pp.
22. Mathur, M.B., 1983: On the use of lower saturation criteria for release of latent heat in NWP models. Mon. Wea. Rev., 111, 1882-1885.
23. Rosenthal, S.L., 1978: Numerical simulation of tropical cyclone development with latent heat release by the resolvable scales. I: Model description and preliminary results. J. Atmos. Sci., 35, 258-271.
24. Frank, W.M., 1983: Review—The cumulus parameterization problem. Mon. Wea. Rev., 111, 1859-1871.
25. Molinari, J., and M. Dudek, 1986: Implicit versus explicit convective heating in numerical weather prediction models. Mon. Wea. Rev., 114, 1822-1831.
26. Kuo, Y-H. and R.A. Anthes, 1984: Semiprognostic tests of Kuo-type cumulus parameterization schemes in an extratropical convective system. Mon. Wea. Rev., 112, 1498-1509.
27. Molinari, J., 1982: A method for calculating the effects of deep convection in numerical models. Mon. Wea. Rev., 110, 1527-1534.
28. Hirt, W.D., 1986: Large precipitation "bull's-eyes" and their effect on the NGM 48 hour forecast. Central Region Tech. Attachment 86-23, National Weather Service, Kansas City, Mo., 7 pp.
29. Koch, S.E., W.C. Skillman, P.J. Kocin, P.J. Wetzel, K.F. Brill, D.A. Keyser and M.C. McCumber, 1985: Synoptic scale forecast skill and systematic errors in the MASS 2.0 model. Mon. Wea. Rev., 113, 1714-1737.

30. Phillips, N.A., 1986b: *Temperature bias in forecasts from the Nested Grid Model. Western Region Tech. Attachment 86-29, National Weather Service, Salt Lake City, UT, 5 pp.*

31. Diak, G., S. Heikkinen and J. Bates, 1986: *The influence of variations in surface treatment on 24-hour forecasts with a limited-area model, including a comparison of modeled and satellite-measured surface temperatures. Mon. Wea. Rev., 114, 215-232.*

32. Ookouchi, Y., M. Segal, R.C. Kessler and R.A. Pielke, 1984: *Evaluation of soil moisture effects on the generation and mod-*

ification of mesoscale circulations. Mon. Wea. Rev., 112, 2281-2292.

33. Benjamin, S.G., 1986: *Some effects of surface heating and topography in the regional severe storm environment. Part II: Two-dimensional idealized experiments. Mon. Wea. Rev., 114, 330-343.*

34. Kaplan, M.L., J.W. Zack, V.C. Wong and C.D. Coats, 1984: *The interactive role of subsynoptic scale jet streak and planetary boundary layer processes in organizing an isolated convective complex. Mon. Wea. Rev., 112, 2212-2238.*

AN ATMOSPHERE OF PROFESSIONALISM.

TASC stands among the world's leading systems engineering organizations, generating solutions for today's complex systems problems through imaginative application of modern analytic tools. Our leadership directly reflects our growth-oriented philosophy and small-team structure that allows for an individualized pursuit of excellence. It's the atmosphere of professionalism that technical individuals everywhere are searching for.

Our current research in the physical and mapping sciences and short-term weather forecasting creates exceptional opportunities for meteorological professionals. Become part of a company that will encourage and sustain your ideas — TASC.

Sr. Meteorologist

Perform meteorological studies, write application programs, design and implement computer systems. Requires PhD in Atmospheric Sciences or a related discipline, knowledge of DEC VAX and PC's, and strong Math/Statistics background. Experience in government meteorological service a plus, as is knowledge of radar and/or satellite meteorology.

Marine Meteorologist

Carry out a variety of computer-based marine meteorological analyses, using DEC VAX and/or IBM PC's. Requires MS in Atmospheric Sciences or closely-related field, at least two years' directly applicable professional experience, and in-depth knowledge of naval and civilian marine studies.

Meteorological Applications Programmer

Design, develop and code software for computer-based workstations in meteorological applications. Requires MSEE or MSCS, 3 years' directly related experience, and knowledge of C programming and computer hardware.

TASC offers a salary philosophy sensitive to accomplishment, participation in a highly successful profit sharing plan, and a broad benefits program. To learn more, send resumes to: Brigitte N. Olivier at the address below.

An Equal Opportunity Employer, M/F.
U.S. Citizenship Required.

TASC
THE ANALYTIC SCIENCES CORPORATION

55 Walkers Brook Drive
Reading, MA 01867
(Route 128 to exit 39)